Synthesis of Graphene Oxide – Polyacrylic Acid Coated Reverse Osmosis Membranes

A Thesis

Presented to

The Faculty of the Department of Chemical Engineering

University of Houston

In Partial Fulfillment

Of the Requirements for the Degree

Bachelor

In Chemical Engineering

By

Tayler Hedtke

May 2019

Synthesis of Graphene Oxide – Polyacrylic Acid Coated Reverse Osmosis Membranes

Tayler Hedtke

Approved:

Chair of the Committee
Dr. Debora Rodrigues, Professor,
Civil and Environmental Engineering

Committee Members:

Dr. Jacinta Conrad, Professor,
Chemical and Biomolecular Engineering

Dr. Frank Claydon, Professor,
Electrical and Computer Engineering

Dr. Suresh K. Khator, Associate Dean,
Cullen College of Engineering

Dr. Michael Harold, Professor and Chair,
Chemical and Biomolecular Engineering

Acknowledgements

I would like to thank those who helped me as I completed my thesis since I would not have made it through this project without them. Dr. Debora Rodrigues agreed to take me on board her research group for the last year and a half and has always been flexible with my other academic commitments. Ali Ansari introduced me to microbial research and continued to assist with sample analysis throughout the project. Janire Peña Bahamonde provided invaluable assistance throughout the past few months especially as the project ran into unexpected difficulties. Lastly, I would like to thank my committee members and the remainder of the Rodrigues research group.

Synthesis of Graphene Oxide – Polyacrylic Acid Coated Reverse Osmosis Membranes

An Abstract

of a

Thesis

Presented to

the Faculty of the Department of Chemical Engineering

University of Houston

In Partial Fulfillment

of the Requirements for the Degree

Bachelor

in Chemical Engineering

by

Tayler Hedtke

December 2016

Abstract

Reverse osmosis (RO) treatment is a practical option for alleviating potable water scarcity. RO is efficient compared to other technologies, and infrastructure is already in place with the opportunity to modify membranes with few complications. One issue plaguing RO is fouling: microbial and mineral, but antifoulants can reduce both types. The respective antifoulants and processes interact, which necessitates further research to understand the processes in relation to each other and to increase RO efficiency.

Two syntheses were investigated to attach graphene oxide (GO) to the membrane. Synthesis One used amination with EDC and NHS, and Synthesis Two used polydopamine (PDA). Synthesis One failed to attach GO to the membrane concluded primarily from FTIR spectroscopy. Synthesis Two was successful based on FTIR and Raman spectroscopy and permeability testing. After Synthesis Two's completion, polyacrylic acid (PAA) was attached to GO through UV light-induced polymerization. Permeability results indicated that the PDA-GO-PAA procedure was a promising synthesis.

Table of Contents

List of Figures

List of Tables

Nomenclature

- DI – deionized
- ED – ethylenediamine
- EDC – N-(3-Dimethylamineopropyl)-N'-ethylcarbodiimide hydrochloride
- FTIR – Fourier transform infrared
- GO – graphene oxide
- HCl – hydrochloric acid
- HEPES – 4-(2-Hydroxyethyl)piperazine-1-ethanesulfonic acid
- M - molarity
- MES – 4-Morpholineethanesulfonic acid
- NaCl – sodium chloride
- $NaHSO_3$ – sodium bisulfite
- NaOCl – sodium hypochlorite
- NaOH – sodium hydroxide
- NHS – N-hydroxysuccinimide
- PAA – polyacrylic acid
- PA-TFC – polyamide-thin film composite
- PDA or PD - polydopamine
- ppm – parts per million
- rpm – revolutions per minute

Section 1: Introduction

Potable Water Scarcity

Potable water scarcity is a significant challenge faced by many regions of the world and is expected to become increasingly problematic in the coming years. Some regions face scarcity due to physical shortages that may be caused by drought or resource overuse, while other regions have access to water that is contaminated above recommended pollutant limits. The combination of the two types of restricted access lead to 1.2 billion people left without access to safe drinking water and millions of deaths annually as a direct result of waterborne diseases and contaminants (Shannon, et al., 2008). The global population is predicted to reach 10 billion by 2050, which will place more substantial demands on infrastructure and water resources, such as aquifers and rivers, that current technologies are not adequately equipped to satisfy (Hegab & Zou, 2015). Increasing population combined with rising living standards could lead to an estimated two-thirds of the global population experiencing water shortage by 2025 (Kim, Ko, Kang, & Han, 2010). Public health efforts, environmental concerns, and increased contamination levels all drive the desire to further purify water that was previously considered satisfactory when current laws and treatment infrastructure were put in place. Industry and the use of products that introduce emerging contaminants, such as engineered chemicals, make water purification more difficult. These combined factors substantially increase the strain on infrastructure dealing with water treatment and transport and may render the use of current technologies unsustainable.

Reverse Osmosis

One of the most promising technologies to help alleviate the issue of potable water scarcity is reverse osmosis (RO) water treatment. RO is a pressure-driven membrane-based water purification technique that removes undesired components from feed water to produce a permeate stream of increased purity. RO operates by having a higher hydrostatic pressure than osmotic pressure. Hydrostatic pressure is directly exerted by a fluid as it presses against a surface, and osmotic pressure is caused by concentration gradients of solutes in a fluid. The membrane acts as a semi-permeable barrier that selectively allows cross-membrane transport of particles. Transport is dependent on the physical properties of both the membrane and the material passing through. Properties of importance include size, polarity, hydrophobicity, and ability to interact with other molecules.

RO's popularity stems from its versatility and efficiency in producing fresh water from both saline water and wastewater sources. Regarding desalination, RO treatment has higher performance than other currently available technologies due to its energy efficiency, low environmental impact, and ease of operation (Elimelech & Phillip, 2011). Opportunities to improve RO technology regarding energy usage and selection efficiency exist for designing future treatment plants or retrofitting new solutions into already active facilities. RO's versatility is in part due to its use of membranes that can be modified with relative ease to enhance the treatment process. The most common type of membrane is the polyamide thin-film composite (PA-TFC) membrane due to its ability to withstand high temperatures, variations in pH, pressure compaction, and biological attacks while retaining high water permeability and selectivity (Liu & Xu, 2016). Unfortunately, PA-

TFC membranes' physiochemical surface properties cause a propensity for degradation by disinfectant chemicals and fouling (Rahaman, et al., 2014). PA-TFC membranes consist of an active polymer layer with interstitial voids, a porous polysulfone support, and a non-woven polyester fabric base. Several different syntheses have been consistently used in the literature and industrial production. The polymer is typically made of either aromatic polyamides or cellulose acetate, and its structure is dense, amorphous, and very thin (Xu, Wang, & Li , 2013). Aromatic polyamide membranes are used in this study.

Fouling

Fouling is the phenomenon of solutes adsorbing onto a membrane's surface or within a membrane's pores. Solute adsorption can occur reversibly or irreversibly. Reversible fouling can be removed from membranes through cleaning procedures, while irreversible fouling remains intact until the membrane is replaced. Fouling is one of the most significant concerns for the RO industry, especially when treating water with high levels of salinity, total dissolved solids, or microorganisms. Fouling decreases both flux and permeate quality leading to increased pressure requirements and energy expenses and decreased membrane life spans. Membrane cleaning and replacement account for up to half of treatment plants' operational costs making research on fouling reduction a potentially valuable investment (Matin, Khan, Zaidi, & Boyce, 2011).

Fouling falls under two major categories: mineral scaling and biofouling. Mineral scaling is the buildup of salts on the membrane. The increase of either the permeate flowrate or purity results in higher mineral salt ion concentrations on the active layer of the membrane. If their concentrations exceed saturation levels, the rates of crystallization and deposition on the membrane can drastically increase. Typical salts that create scaling issues are calcium sulfate (gypsum), calcium carbonate, calcium phosphate, barium sulfate, and silica (Lyster, Kim, Au, & Cohen, 2010). Polymer antiscalants prevent salt precipitation by adsorbing to crystal surfaces and stopping the formation of crystals larger than the critical size for nucleation or modifying the surface of large crystals (Sweity, Oren, Ronen, & Hersberg, 2013). Polymer antiscalants are typically composed of polyacrylic acid, carboxylic acid, or phosphonates and are dosed into feed water as a free-floating substance that will not pass through the membrane, but they can also be attached to the membrane surface (Lyster, Kim, Au, & Cohen, 2010). Polyacrylic acid (PAA) is the polymer antiscalant used in this study. Low enough concentration must be used to avoid increasing fouling rates or blocked pores.

Biofouling is the formation of biofilm, a structure of surface-associated microbial cells attached to a surface held together in a matrix of extracellular polymeric substances (EPS) (Matin, Khan, Zaidi, & Boyce, 2011). EPS accounts for between 50 and 90% of the total organic carbon in biofilms and is composed of macromolecules generated by microorganisms. Biofilm builds up as microorganisms die and remain held together by the EPS while new cells grow above them sustained by feed water carrying a continuous stream of nutrients. Sections of the biofilm eventually break off, but most of the biofilm's mass is irreversible fouling. Pretreatment with disinfectants, such as chlorine, is a standard countermeasure to reduce biofouling. Unfortunately, pretreatment alone cannot eradicate biofouling because its effectiveness never reaches 100% microbial death. Any surviving microorganisms then continue to reproduce and relocate (Matin, Khan, Zaidi,

& Boyce, 2011). Chlorine and other pretreatment compounds must be used in moderation at less effective levels when used with PA-TFC membranes to prevent degradation of the PA layer (Liu & Xu, 2016). Thus, additional methods of biofilm control must be explored to increase RO efficiency.

Membrane coatings are one solution for biofilm reduction. Compounds with various functional groups can be attached to the active layer of membranes with chemical reactions. The new functional groups alter membrane surface properties that affect foulant behavior. Graphene oxide (GO) is a popular compound for modifying membranes and is the focus of this study. GO has antimicrobial properties that kill microorganisms through direct contact causing cell membrane stress from the GO nanosheets' sharp edges followed by superoxide anion-independent oxidation (Liu, et al., 2011) (Hegab & Zou, 2015). In addition to having antimicrobial properties, GO has other characteristics that make it an attractive option for membrane surface modification: high mechanical strength, chemical inertness, microscale thickness, smoothness, hydrophilicity, negative surface charge, and easy manufacturing (Liu & Xu, 2016). GO stays attached to the membrane during the treatment process, unlike released biocides, resulting in constant effectiveness throughout the lifetime of the membrane. Surface functionalization of RO membranes is a relatively new concept that has developed over the last several years and has produced promising results (Perreault, Tousley, & Elimelech, 2014).

Interactions between Fouling Mechanisms and Antifoulants

Mineral scaling and biofouling are often viewed as individual concerns in laboratory testing, but their interactions must also be considered for applications with realistic feed composition. A set of interactions arise when salts, microorganisms, antifoulants, and membrane coatings are combined in a single system and subsets of their interactions have become popular in contemporary RO research.

Biofilm formation can create a feedback loop that increases the rate of mineral scaling. Numerous studies have found that flux decline is sped up when microorganisms and mineral salts are both present in feed water as compared to when only one is present. Biofouling can enhance additional mineral salt deposition through the mechanism of microorganisms serving as crystal nuclei that induce crystallization (Hou, Gao, Li, & Xu, 2010). Another mechanistic possibility is that salt saturation is enhanced in and near biofilms creating conditions more favorable for crystallization than those in feed water contacting a clean membrane (Radu, Bergwerff, van Loosdrecht, & Picioreanu, 2015). Additionally, each type of fouling's specific antifoulant has an impact on the rate of both mineral and microorganism buildup.

GO modification on a membrane surface purposely targets microorganisms but also affects mineral scaling. GO has been shown to inhibit scaling of negatively charged salts, such as gypsum, by giving the membrane a negative charge that creates charge repulsion (Cao, Ansari, Yi, Rodrigues, & Hu, 2018). While GO decreases mineral scaling, polymer antiscalants increase the rate of biofouling. The presence of antiscalants in feed water can increase biofilm growth by increasing microbial growth rates by up to ten times the normal growth rate by serving as a food source or altering the membrane surface (Sweity, Oren, Ronen, & Hersberg, 2013). Antiscalants serve as a carbon and phosphorous source under limited nutrient conditions as well as increase membrane hydrophobicity which aids microorganism attachment.

Section 2: Methods and Materials

Materials and Chemicals

Synthesis One was performed with a commercial PA-TFC reverse osmosis membrane (ESPA2, Hydranautics Inc. Oceanside, CA), isopropanol (≥99.5%, Sigma Aldrich), sodium hypochlorite (NaOCl; 10-15% Cl available, Sigma Aldrich), sodium bisulfite ($NaHSO_3$; Fisher Scientific), 4-Morpholineethanesulfonic acid monohydrate (MES monohydrate; 98%, Alfa Aesar), Ethylenediamine (ED; 99%, Acros Organics), N-(3-Dimethylamineopropyl)-N'-ethylcarbodiimide hydrochloride (EDC; 98+%, Acros Organics), N-hydroxysuccinimide (NHS; 98+%, Acros Organics), sodium chloride (NaCl; J.T. Baker Inc), 4-(2-Hydroxyethyl)piperazine-1-ethanesulfonic acid (HEPES; 99%, Acros Organics), graphene oxide (synthesized from graphite: <20 µm, Sigma Aldrich), HCl (1 M), NaOH (0.1 M), and deionized water (DI water; Ultrapure purification system).

Synthesis Two was performed with a commercial TFC polyamide reverse osmosis membrane (ESPA2, Hydranautics Inc. Oceanside, CA), isopropanol (≥99.5%, Sigma Aldrich), dopamine hydrochloride (Sigma Aldrich), Tris-HCl (pH 7.2, 1 M, Sigma Aldrich), graphene oxide (synthesized from graphite: <20 µm, Sigma Aldrich), hydrochloric acid (HCl; 1 M), sodium hydroxide (NaOH; 0.1 M), and deionized water (DI water; Ultrapure purification system).

The Polyacrylic Acid (PAA) addition was performed with polydopamine-GO modified membranes and acrylic acid monomer (99%, Sigma Aldrich).

Graphene Oxide Preparation

The GO nanosheets were prepared from graphite using the Hummer's method. In brief, graphite was oxidized by adding concentrated sulfuric acid (H_2SO_4), sodium nitrate ($NaNO_3$), and potassium permanganate ($KMnO_4$) and then cooled overnight. After cooling, DI water was added, and the solution was heated. Additional DI water along with diluted hydrogen peroxide (H_2O_2) was added slowly. The solution was then sonicated, settled, decanted, and dried before the solid was stored for use. Further details can be found in (Cao, Ansari, Yi, Rodrigues, & Hu, 2018).

General Synthesis Information

Syntheses

While additional syntheses were briefly explored, two primary synthesis procedures were emphasized: Synthesis One using EDC and NHS to link GO to the membrane and Synthesis Two using polydopamine to link GO to the membrane.

Membrane size considerations

Initial syntheses used small pieces of membrane cut roughly to the dimensions of 2.5 in x 3 in. Membranes of this size used 10-15 mL of solution to adequately cover the surface during reactions. Larger membranes, cut to roughly the dimensions of 15 in. x 10 in., required increased solution volumes to account for raised portions of the membrane. Occasionally, evaporation or small leaks during longer duration reactions caused raised portions of the membrane surface to become exposed. The exposed regions were avoided when cutting the membrane into smaller sections for testing if the synthesized membrane was large or the entire membrane was discarded if the synthesized membrane was small. Small membrane samples were initially used to avoid wasting materials while the modified membranes were tested for surface characterization using analytical instruments. Larger membrane samples were synthesized once data supported synthesis completion to allow for comparison samples for membrane homogeneity.

Membrane storage

Membrane samples must be kept moist to retain their functionality. Before use, the membranes were covered in DI water and stored in a refrigerator. After a synthesis was completed, the membrane samples were returned to the same storage conditions. For FTIR spectroscopy analysis or other composition tests, the membrane samples must be dry to prevent water molecules from affecting the results. The samples were dried either by air-drying overnight or freeze-drying if a shorter time period was desired.

Isopropanol use

After the initial Synthesis One trials failed, the literature was examined to search for potential solutions. Based on several journal articles, the first step of all syntheses became contacting the membrane with pure isopropanol on a shaker plate to remove any potential contaminants from the membrane surface.

Synthesis One – EDC/NHS Graphene Oxide Membrane Synthesis

The first synthesis for attaching GO to a PA-TFC membrane used EDC and NHS as the primary reactants to modify the active polyamide layer and attach GO through amination (Perreault, Tousley, & Elimelech, 2014). The reaction steps of the synthesis are outlined in Figure 1. The synthesis is presented in its final form based on results from initial experiments.

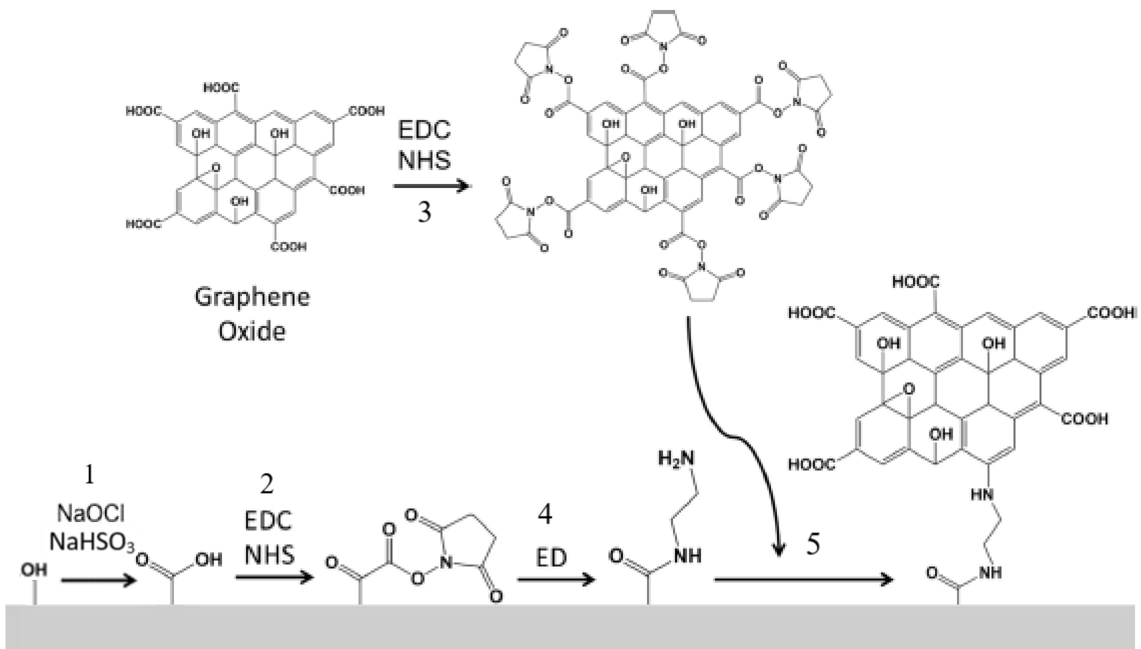

Figure 1: Reaction steps for Synthesis One. Step 1 adds NaOCl, rinses, and adds $NaHSO_3$. Step 2 functionalizes the membrane with EDC and NHS. Step 3 activates the graphene oxide (GO) with EDC and NHS. Step 4 functionalizes the membrane with ED. Step 5 attaches the activated GO to the ED functionalized membrane.

A PA-TFC membrane was prepared for the synthesis by placing it in a foam frame. Metal clips held the membrane to an aluminum foil back exposing only the active side of the membrane to the solutions poured into the frame. All reactions took place with enough solution to cover the membrane surface. For the initial syntheses with small sample areas, 10-15 mL was adequate. The membrane was contacted with pure isopropanol for one hour on a shaker plate at 90 rpm to remove preservatives and other materials from storage solutions from the membrane surface. The membrane was then rinsed with DI water.

Step 1 converted the native hydroxyl (-OH) groups into carboxyl (-COOH) groups. The membrane was contacted with pure NaOCl for five minutes on a shaker plate at 90 rpm. The reaction time was optimized by performing this step with multiple lengths (2, 5, and 30 min.) and characterizing the resulting membrane surface with FTIR spectroscopy. The results are summarized in Table 1.

Table 1: FTIR spectroscopy summary for variations in step 1 of Synthesis One.

Reaction Time (min)	Functionalization
2	Low
5	High
30	High

Five minutes and 30 minutes both provided greater functionalization than two minutes. Since there was not evidence of 30 minutes being more effective than five minutes, five minutes was selected as the reaction time for the remaining trials. After five minutes, the membrane was rinsed with DI water. Then, the membrane was contacted with 1000 ppm $NaHSO_3$ for 30 seconds before rinsing well with DI water.

Step 2 added amide-ester functionalization to the membrane surface. The membrane was contacted with a 10 mM MES buffer solution containing 4 mM EDC, 10 mM NHS, and 0.5 M NaCl for two hours on a shaker plate at 90 rpm. Before contact, the pH should be adjusted to 5 if needed. EDC and NHS were the reactants and NaCl kept the ion concentration near constant in the solution. After the reaction was complete, the membrane was rinsed with DI water.

Step 3 activated the GO to prepare it for attachment to the membrane surface. The GO was in solution at 1000 ppm in 10 mM MES buffer. To ensure even GO dispersion, the solution was probe sonicated for 10 minutes. Next, 2 mM EDC and 5 mM NHS were added to the GO solution, and the pH was adjusted to 5.5 and placed on a magnetic stir plate for at least 15 minutes of reaction time.

Step 4 added amine functionalization to the membrane surface. A solution containing 10 mM HEPES buffer in DI water and 0.15 M NaCl and 60 μg ED with a pH adjusted to 7.5 was contacted with the membrane for one hour on a shaker plate at 90 rpm. After the reaction, the membrane was rinsed with DI water.

Step 5 functionalized the membrane surface with activated GO. The GO solution from Step 3 was adjusted to pH 7.2 and then contacted with the membrane for 2.5 hours on a shaker plate at 90 rpm. After the reaction, the membrane was removed from the frame and both sides were rinsed with DI water. Depending on the synthesized membrane's final purpose, the membrane was either dried or stored in DI water.

Synthesis Two – Graphene Oxide Polydopamine Membrane Synthesis

The second synthesis for attaching GO to a PA-TFC membrane functionalized the membrane with PDA and then attached GO to the PDA (Zhang, Jia, Qiu, & Pan, 2018) (Rao, Feng, Tang, & Wu, 2016) (Li, Peng, Luo, & Yu, 2015). The steps for Synthesis Two are shown in Figure 2.

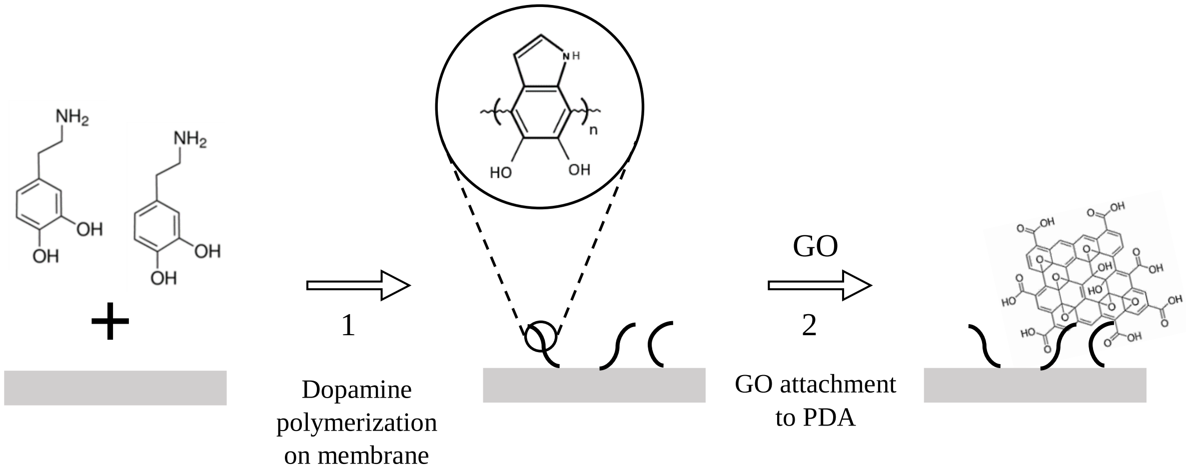

Figure 2: Series of reactions for Synthesis Two.

The PA-TFC membrane was prepared for the synthesis in the same way as for Synthesis One. The membrane was placed in a foam frame before being contacted with pure isopropanol for one hour on a shaker plate at 90 rpm and then rinsed with DI water.

<u>Step 1</u> added polydopamine chains to the membrane surface. A 2.0 g/L solution of dopamine hydrochloride in Tris buffer at pH 8.5 was made and then contacted with the membrane for two hours on a shaker plate at 90 rpm before rinsing with DI water. The solution gradually changed in color from clear to black or dark brown during the reaction. Polydopamine chains are composed of dopamine monomer units with the chemical structure shown in Figure 3 that also attach to functional groups on the membrane surface.

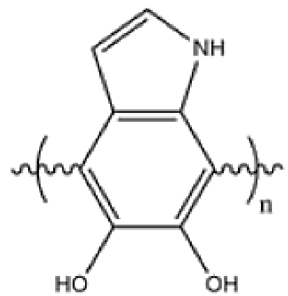

Figure 3: Dopamine monomer in a polydopamine chain.

Step 2 added GO to the polydopamine-coated surface. GO was added to Tris buffer at 1000 ppm and probe sonicated for 10 minutes to ensure even dispersion. The mixture was then contacted with the membrane for one hour on a shaker plate at 90 rpm before being rinsed with DI water.

Attaching Polyacrylic Acid

After GO was attached to the membrane's surface, PAA was added to the GO nanosheets. The acrylic acid monomer was contacted with the PDA/GO modified membrane surface with enough solution volume to cover the entire surface and then placed under UV light. Microwaves can also induce polymerization, but UV light was the selected method because the foam frames could not withstand the required time in the microwave. The extent of polymerization should increase with longer reaction times. The monomer unit structure in PAA is shown in Figure 4. Excessive polymerization blocks the membrane's pores resulting in reduced permeability, but not enough polymerization limits the antiscalant's effectiveness.

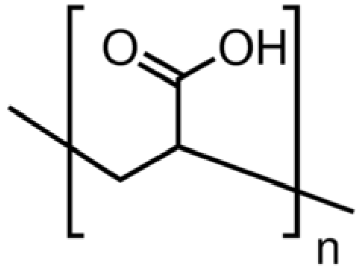

Figure 4: Acrylic acid monomer in a polyacrylic acid chain.

Analytical Tests

<u>Visible changes</u>

The simplest indication of reactions is visual changes on the surface. For example, the dopamine solution in contact with the membrane significantly darkens in color as polymerization occurs during Synthesis Two. The membrane surface also becomes discolored in the contact area as the synthesis progresses as seen in Figure 5.

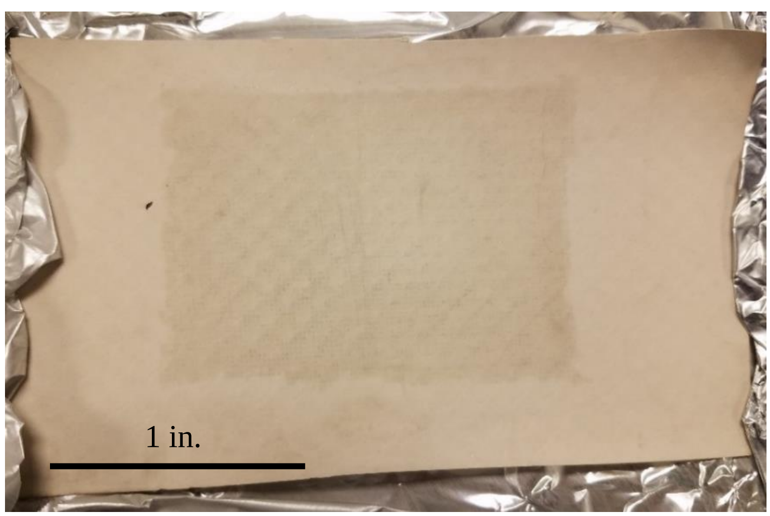

Figure 5: PA-TFC membrane after step 2 of Synthesis One.

A dark-colored rectangle appears in the middle of the membrane where it was exposed to reactant solutions. Unfortunately, the visual changes to the membranes cannot be linked to the desired chemical modifications meaning that further analytical techniques are required. For example, the addition of a GO layer should not be expected to change the appearance of the membrane surface (Perreault, Tousley, & Elimelech, 2014).

Fourier-transform infrared spectroscopy (FTIR)

FTIR spectroscopy is a tool used to identify the chemical structure of materials. Chemical functional groups are identified by their characteristic absorption of infrared radiation, which is shown as local minima at particular wavenumbers. Peak depth or intensity is affected by both the type of bond corresponding to the peak and by the number of bonds present in the sample. The wavenumbers used to analyze the membrane samples were in the range of 4000 to 640 cm^{-1}. The graphs show intensity vs wavenumber. Intensity is measured in arbitrary units (a.u.), and the actual value peak intensity does not matter, except in relation to other peaks. Thus, individual curves can be vertically shifted without altering the validity of the data; curves are often shifted to make comparisons on the same graph more easily viewed. While relative intensity carries significance, a peak's depth is not able to be directly translated to a calculated bond quantity.

Confocal microscopy

Confocal microscopy is a variant of fluorescence microscopy that creates high-resolution, three-dimensional images of materials stained with fluorescent molecules. Confocal microscopy allows biofilms to be analyzed throughout their depth. Biofilms are stained with both red and green fluorescing dyes. The red dye selectively stains dead cells in the film, while the green dye selectively stains living cells in the film. The two colors are detected in separate scans by switching the wavelength used to excite the fluorophores. The biofilm can be scanned from its surface to its base by altering the focus of the microscope, allowing the biofilm's volume to be calculated along with the ratio of living to dead cells.

Raman spectroscopy

Raman spectroscopy analyzes the chemical composition of materials by detecting vibrations involving a change in polarizability of molecules. Rather than observing absorption like in FTIR spectroscopy, Raman is based on inelastic scattering and the two methods are complementary technologies. Samples are easy to damage during spectroscopy creating unreliable results. Data from different samples are compared by looking at relative peak ratios for different shift values.

Permeability testing

A membrane sample's permeability is a measure of its flux per area per time unit. Permeability was measured by placing the membrane in a laboratory scale RO system, measuring the permeate flow rate, and dividing the rate by the membrane area. The system should be run for a period of time before collecting measurements to allow for membrane compaction as pressurized water flows through it. This study ran the system for one hour before collecting a measurement. Permeability is a function of several membrane characteristics, but one with the most significant impact is pore size.

Section 3: Results and Discussion

Synthesis One was first completed closely following the steps outlined in the literature (Perreault, Tousley, & Elimelech, 2014). The resulting membrane was tested with FTIR spectroscopy, and the results showed no obvious changes from the bare ESPA2 membrane, signifying that the synthesis was unsuccessful. The FTIR spectroscopy result for the bare membrane is shown in Figure 6.

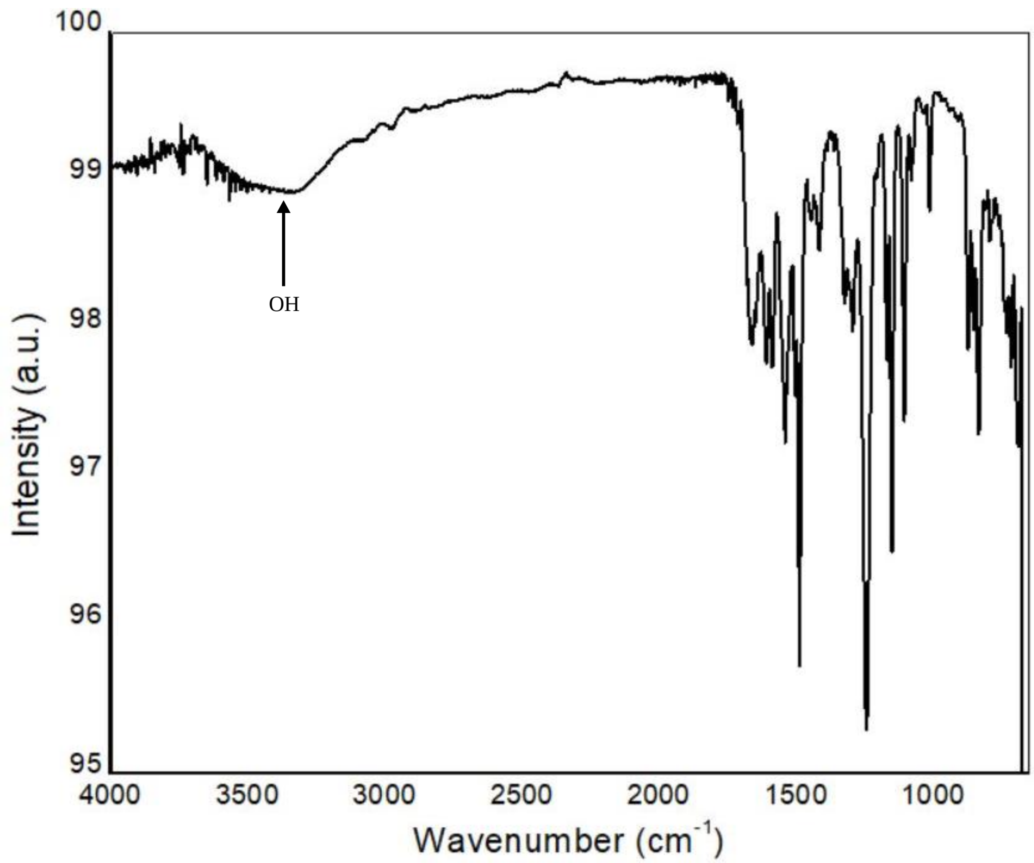

Figure 6: FTIR spectroscopy for the bare ESPA2 membrane as a reference measurement.

The arrow marks the hydroxyl bond (O-H) peak that will be referenced later in the text. Throughout all the syntheses, the hydroxyl peak should stay nearly constant. A substantial change in the shape or intensity signifies an undesired reaction, a wet sample, or the presence of unreacted molecules that should have been removed during DI water rinses between synthesis steps.

After determining that the first trial of Synthesis One was unsuccessful, the procedure was modified. The first reaction step was examined since FTIR spectroscopy was unchanged, which indicated that no reactions took place on the membrane surface. The contact time for step 1 with the membrane and NaOCl was varied for three samples (2, 5, and 30 min.). The membranes were then analyzed with FTIR spectroscopy, and the results are shown in Figure 7 and Figure 8.

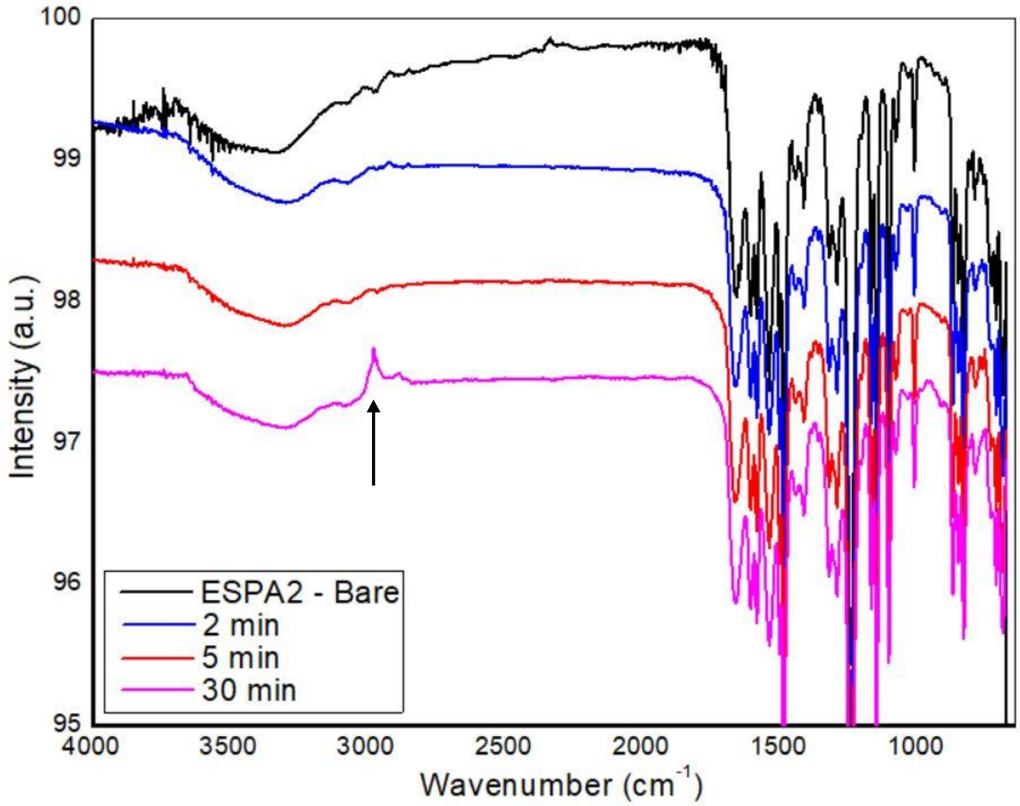

Figure 7: FTIR spectroscopy for the NaOCl reaction of Synthesis One for 2, 5, and 30 minutes along with the bare membrane.

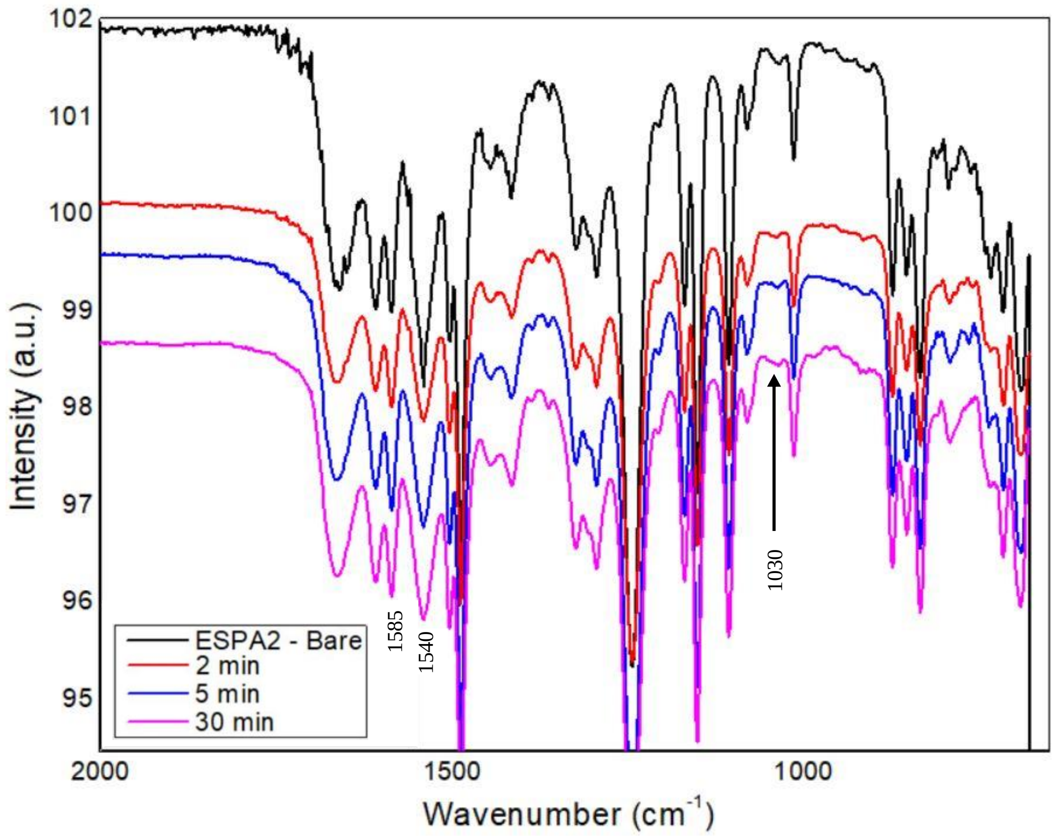

Figure 8: Enlarged view of the low wavenumber portion of Figure 7 for the NaOCL reaction of Synthesis One.

The arrow at 2980 cm^{-1} on Figure 7 shows a local maximum that is not present on the other samples. Inverted peaks, pointing upward, are the result of an issue with the background reading and are not a result of the sample properties. The change of peak intensities at 1585 and 1540 cm^{-1} on Figure 8 suggest that the NaOCl reaction took place since functional groups changed on the membrane surface. All three reaction samples see a slight increase in peak depth at 1585 cm^{-1} and a decrease in peak depth at 1540 cm^{-1}. All three samples also have a shallower peak at 1030 cm^{-1} than the bare membrane. These changes in the data suggest that the reaction is taking place for all time options without adverse effects to the overall membrane structure for longer times.

Another potential source of error in the synthesis was that the GO was not modified and, therefore, was unable to attach to the membrane's amine group. The modified and fresh GO were compared using FTIR spectroscopy. The results are shown in Figure 9.

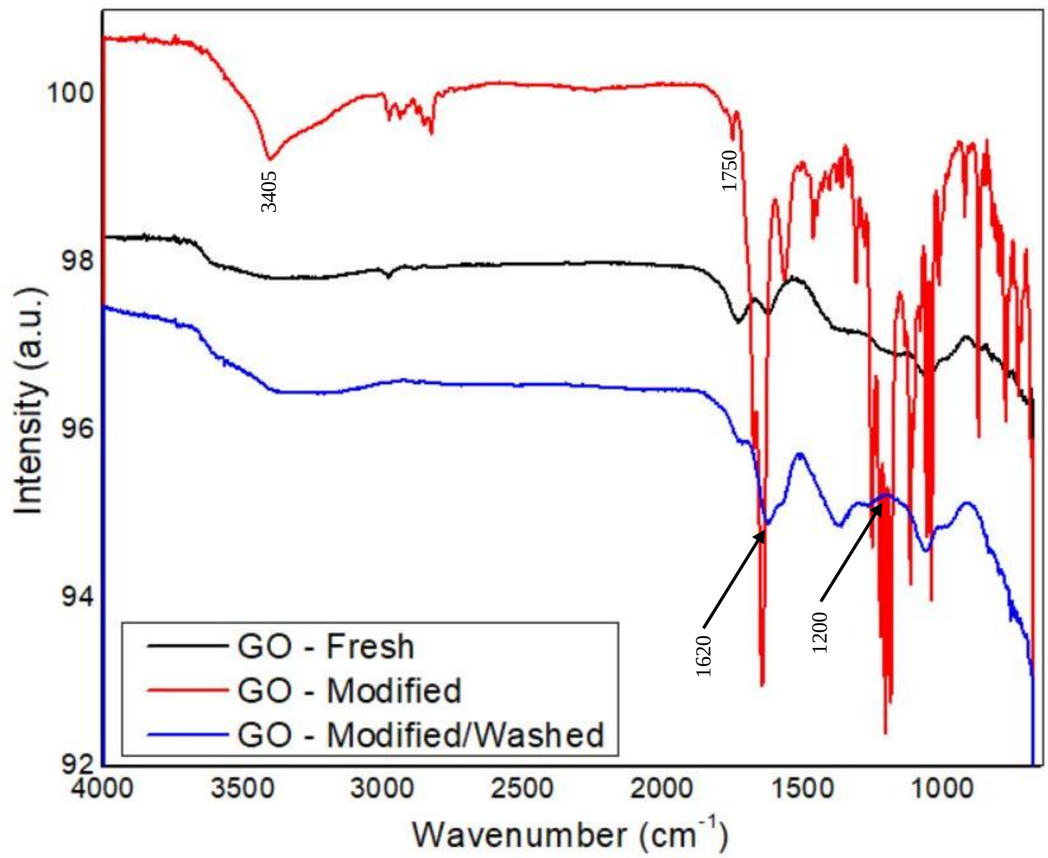

Figure 9: FTIR spectroscopy of fresh graphene oxide (GO), GO modified with NHS/EDC, and modified/washed GO.

The modified GO, the top curve, exhibits numerous unexpected peaks. The hydroxyl peak should not have been significantly altered at 3405 cm^{-1}, and the series of peaks to the right of 1750 cm^{-1} should not be so jagged. The GO sample was assumed to contain unreacted compounds, so the sample was washed, centrifuged, and freeze-dried to remove undesired molecules from the sample before reanalyzing with FTIR. This data set shows the importance of washing samples between reaction steps to remove unreacted compounds and prevent them from interfering with later synthesis steps.

The modified and washed GO sample, the bottom curve, is the data that should be compared to the fresh GO data. The creation of the peak at 1620 cm^{-1} corresponds to the formation of the amide C=O bond that can be seen after the step 3 reactions with EDC and NHS of Synthesis One. The changes to the curves surround the high point at 1200 cm^{-1} also indicate changes to the surface structure. This data set suggests that the GO was successfully modified and that the synthesis' progress was blocked at a different step.

Since the GO was thought to have been modified, a step earlier in the synthesis was checked, the product of step 4. Based on the data from Figure 7 and Figure 8 showing membrane surface changes after two minutes, Synthesis One was carried out using the two-minute reaction time in step 1 with NaOCl. This trial, along with the previous trials, used the recommended concentration of 200 ppm NaOCl. One sample went through the step 1 reactions with NaOCl and $NaHSO_3$, as a control, to ensure that step 1 was still successful. The second sample went through the step 4 reaction with ED. The FTIR for these two samples, along with the bare membrane, are shown in Figure 10.

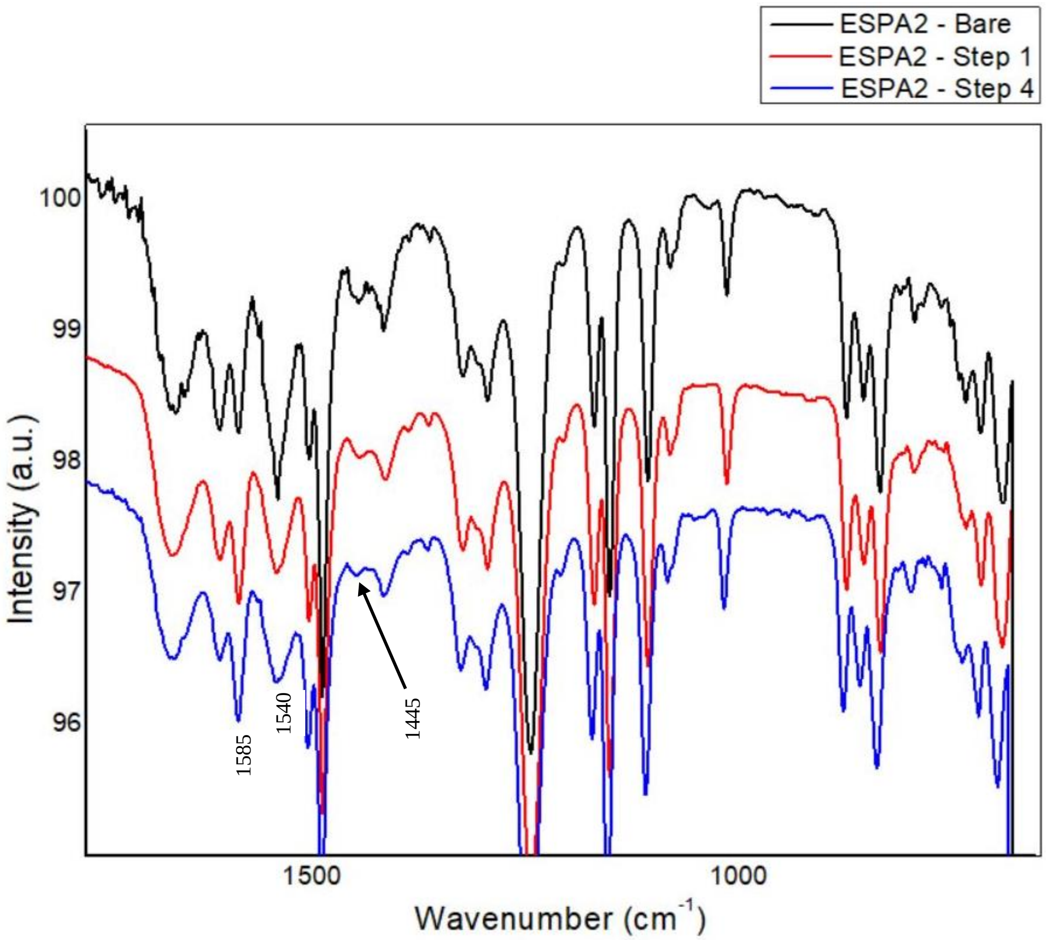

Figure 10: FTIR spectroscopy of the low wavenumber portion of the spectrum for Synthesis One. The bare membrane is compared with the modified membrane after two different reaction steps using a two-minute NaOCl reaction time.

The FTIR spectroscopy shows a change in the membrane surface functionalization between the bare membrane and the modified membrane after step 1. The peak at 1445 cm^{-1} became less distinct. The changes from the bare membrane to after step 1 that surrounded the peaks at 1585 and 1540 cm^{-1} are the same as discussed for Figure 8. The curves are not identical since an additional reaction with H_2SO_4 took place. The presence of surface characteristic changes along with the similarity to the previous trial suggests that both reactions (NaOCl and $NaHSO_3$) of step 1 occurred.

Unfortunately, no significant changes to the data appear after the completion of step 4, indicating that the surface group amination with ED was unsuccessful. One possibility for the failure was that step 2's reaction did not take place because the NaOCl reaction had a low yield, which resulted in a low conversion of hydroxyl groups to carboxylic acid groups. To examine this possibility, the reaction time for the NaOCl reaction was extended to five minutes, and the concentration of NaOCl was increased drastically by using pure reactant. The results of this synthesis are shown in Figure 11.

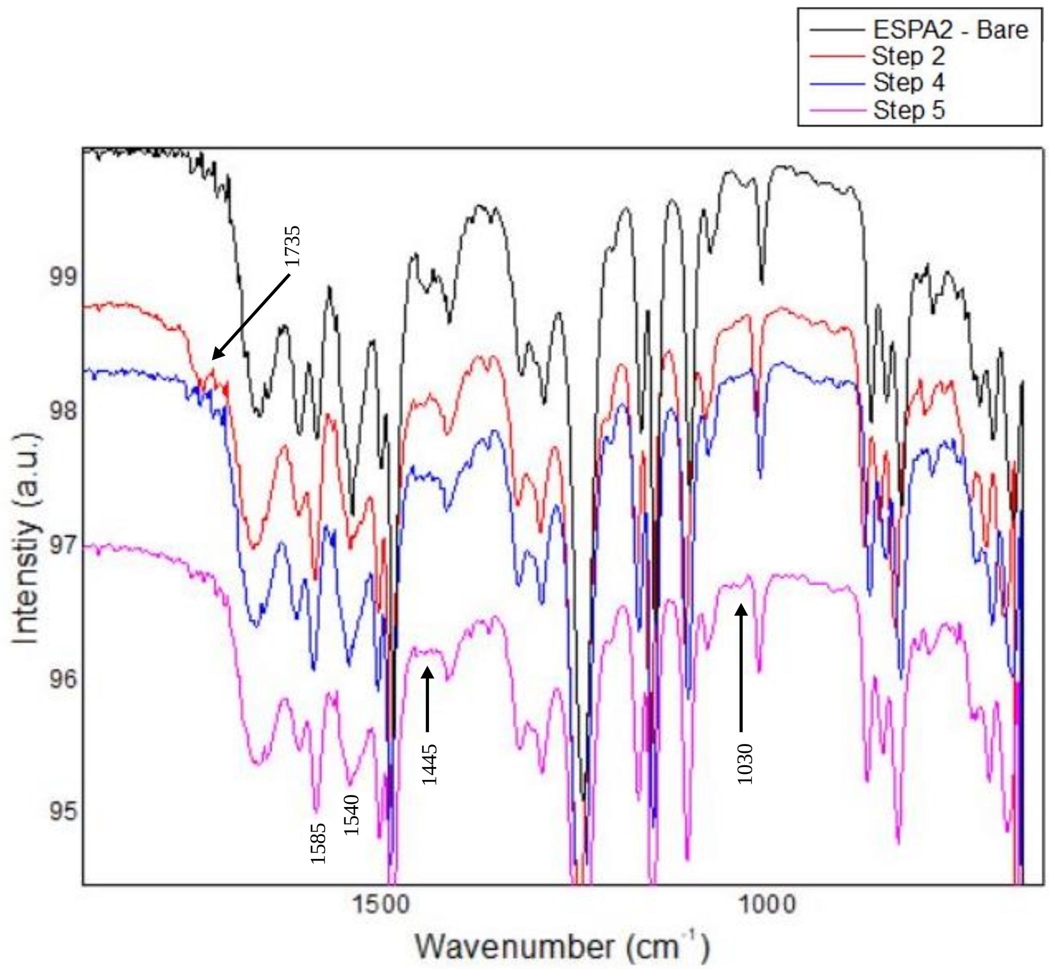

Figure 11: FTIR spectroscopy of the low wavenumber portion of the spectrum for Synthesis One. The bare membrane is compared with the modified membrane after completing 3 different reaction steps using a 5-minute NaOCl reaction time.

This synthesis shows improvement over previous trials with the changes between the bare membrane and the sample for step 2 reactions with EDC and NHS. The peak at 1735 cm^{-1} on the step 2 curve corresponds to the presence of the amide C=O bond in reactive amine-ester functional groups on the membrane surface. This peak disappears for te step 4 sample when the amide C=O bond is removed. The structure of a reactive amine-ester is shown in Figure 12.

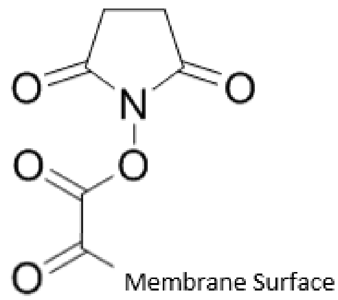

Figure 12: Structure of the reactive amine-esters attached to the membrane surface as the product of step 2.

Changes to the FTIR curves when compared to previous steps for the peaks at 1585, 1540, 1445, and 1030 cm^{-1} are similar to those previously discussed with previous Synthesis One trials regarding the samples for the bare membrane, step 2 and step 4. Step 5 may have succeeded as indicated by the change in depth for the peak at 1540 cm^{-1} and the slope leveling to the left of 1030 cm^{-1} when compared to the step 4 curve. Overall, the changes in FTIR spectroscopy are not strong enough to definitively establish sufficient GO attachment. Raman spectroscopy could be utilized to gain further insight into the chemical makeup of the membrane surface. The instrument was unavailable at this point of the project but was utilized for later trials.

The failure of Synthesis One to be completed could be due to many factors. One factor was that several research groups that performed similar syntheses fabricated their own membrane as the first step of their synthesis. This study used a commercial membrane and, therefore, the active layer of the membrane could have other unspecified functional groups or modifications not reacting well with the reagents used in the synthesis. Despite cleaning the membrane surface with isopropanol, the possibility of unknown surface structures or functional groups remained present.

Since the cause of the error was unknown, alternate syntheses were attempted. A layer-by-layer synthesis was based on the literature and used the ESPA2 membrane (Choi, Choi, Bang, & Lee, 2013). The layers were composed of alternately charged GO layers with the first layer directly attached to the membrane surface without prior modification. The first layer was GO activated by ED and EDC at pH 11, and the second layer was GO at pH 3. This synthesis yielded results similar to those of Synthesis One.

Synthesis Two was next attempted with the ESPA2 membrane as outlined in Materials and Methods. FTIR spectroscopy for the steps of Synthesis Two are shown in Figure 13.

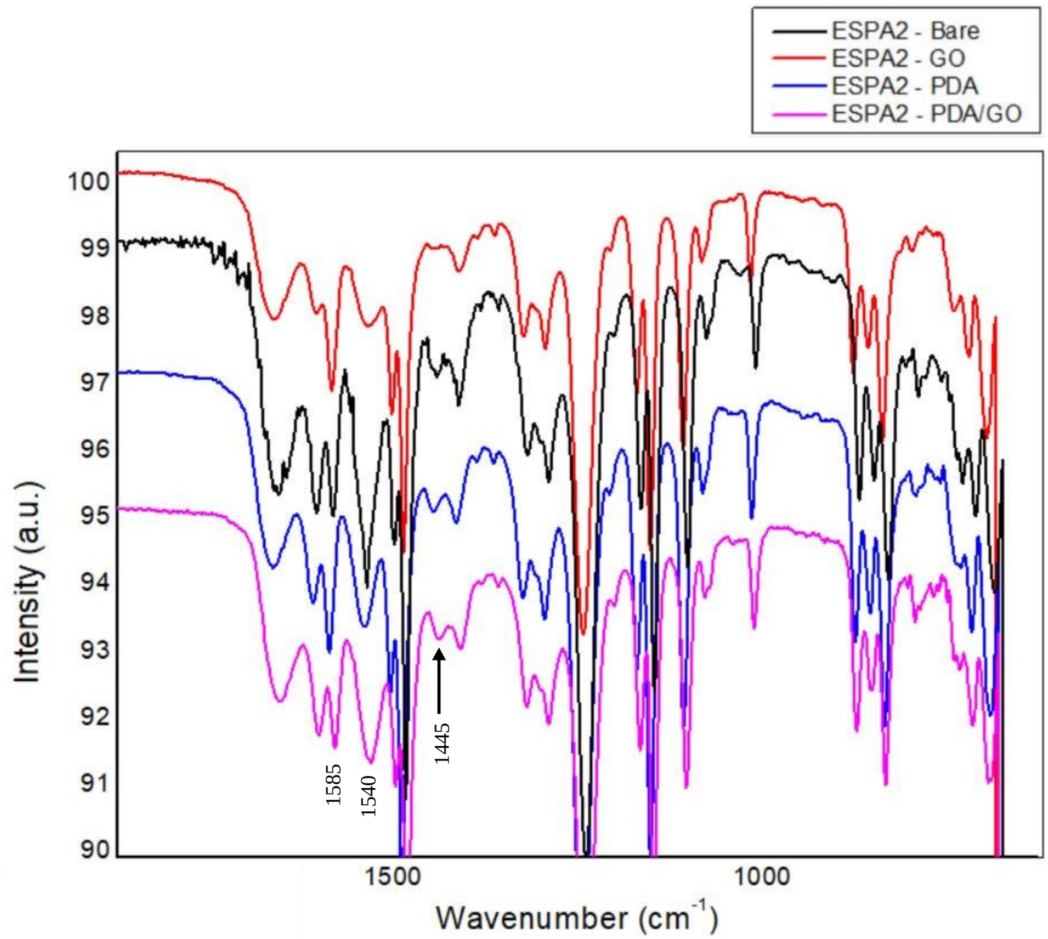

Figure 13: FTIR for the low wavenumber portion of the spectrum for the ESPA2 membrane bare and modified with graphene oxide (GO), polydopamine (PDA), and PDA/GO.

The depths of the peaks at 1585 and 1540 cm^{-1} changed with the addition of PDA and GO (the bottom two curves) compared to the bare membrane and each other. Additionally, the peak at 1445 cm^{-1} changes from the bare membrane in comparison to each of the other samples. These changes suggest that Synthesis Two was successful through the addition of GO. While changes to the surface functional groups are evident, the exact changes were difficult to identify using only FTIR spectroscopy, so Raman spectroscopy was also used to determine if GO attached to the PDA layer. Raman spectroscopy results are shown in Figure 14.

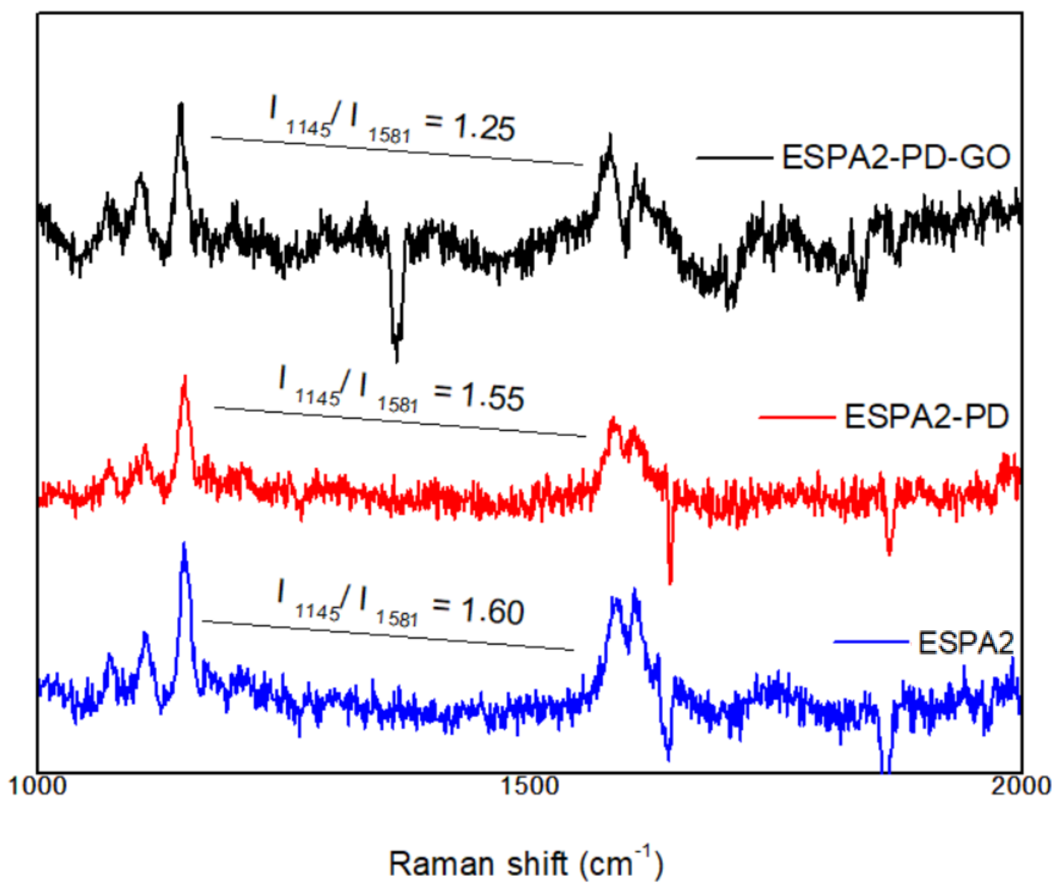

Figure 14: Raman spectroscopy data for the ESPA2 membrane bare and modified with PDA and PDA/GO.

The Raman shift data were analyzed following the literature as shown in (Perreault, Tousley, & Elimelech, 2014). The peak ratio of the shifts at 1145 and 1581 cm^{-1} was compared for the bare membrane, the membrane with only PDA, and the membrane with PDA and GO. Although the peak ratios are changing relative to samples of previous stages of the synthesis, the decrease from the bare membrane to the membrane with PDA and GO should be more substantial to conclusively state that GO has attached. Ideally, the curves would be smoother since the noise in the data detracts from its reliability.

Confocal microscopy was also used to test for GO's presence and antimicrobial effectiveness on the membrane surface. One sample of bare membrane was tested as a control to compare against the sample modified by PDA and GO. The results for the bare membrane are shown in Figure 15 (a) and (b).

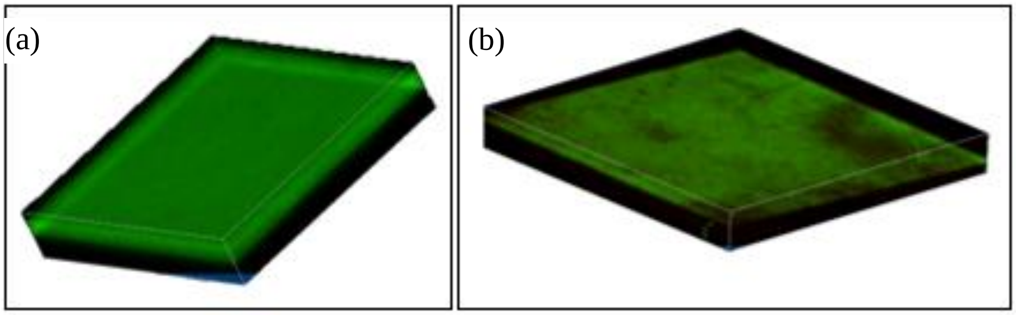

Figure 15: Confocal spectroscopy for the green channel for a bare ESPA2 membrane as a control.

The results of the green channel scan show the presence of many living microorganisms. The red channel scan did not detect positive data points, which means that there were few dead bacteria in the biofilm. To compare with the control sample, the results for the modified membrane are shown in Figure 16 (a) and (b).

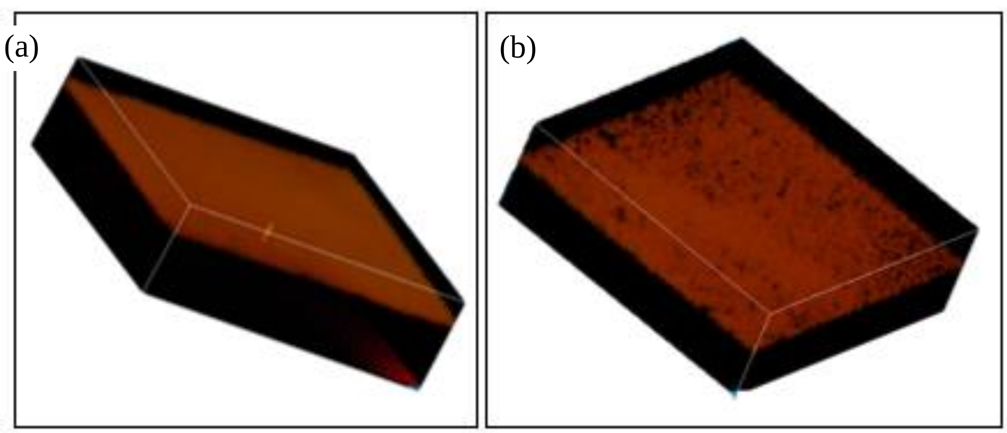

Figure 16: Confocal spectroscopy for the red channel for an ESPA2 membrane modified with polydopamine and graphene oxide.

For the modified membrane sample, the opposite results were found as compared to the control sample. The green channel scan did not detect positive data points, while the red channel scan showed the presence of many dead microorganisms. PDA is not known to have antimicrobial properties, whereas many studies have concluded that GO does have antimicrobial properties (Hegab & Zou, 2015) (Liu & Xu, 2016) (Liu, et al., 2011). The difference in confocal spectroscopy results between the two samples supports the claim that GO attached to the PDA modified membrane surface.

The next test implemented to support GO attachment and check synthesis viability to create a usable modified membrane was measuring permeability. The test was conducted by placing a membrane sample in the RO system for one hour while water is circulated through the system by a pump. The measurements are shown in Table 2. At this point in the study, replicates have not been tested and error has not been calculated. These factors mean that the data are preliminary without replicates or error estimates and act only as supporting evidence rather than definitive findings.

Table 2: Preliminary Synthesis Two permeability test results.

Sample	Permeability (L/m^2-h)
ESPA2	1286
ESPA2 – PDA	1286
ESPA2 – PDA – GO	1224

The addition of PDA to the membrane did not reduce permeability. This suggests that PDA is a viable option for facilitating the attachment of GO to the membrane without blocking pores. When GO is attached to the PDA layer of the modified membrane, permeability is reduced by <5% which is an acceptable amount of decrease. The decrease is larger than for adding PDA alone to the membrane, which signifies that a surface modification took place. The combination of data from FTIR spectroscopy, Raman spectroscopy, and the permeability test demonstrated successful attachment of GO to PDA to create a modified membrane.

Now that the antiscalant targeting biofouling, GO, has been attached, the antiscalant targeting mineral scaling, PAA, can also be incorporated. The results of the additional step are shown in Figure 17 and Figure 18.

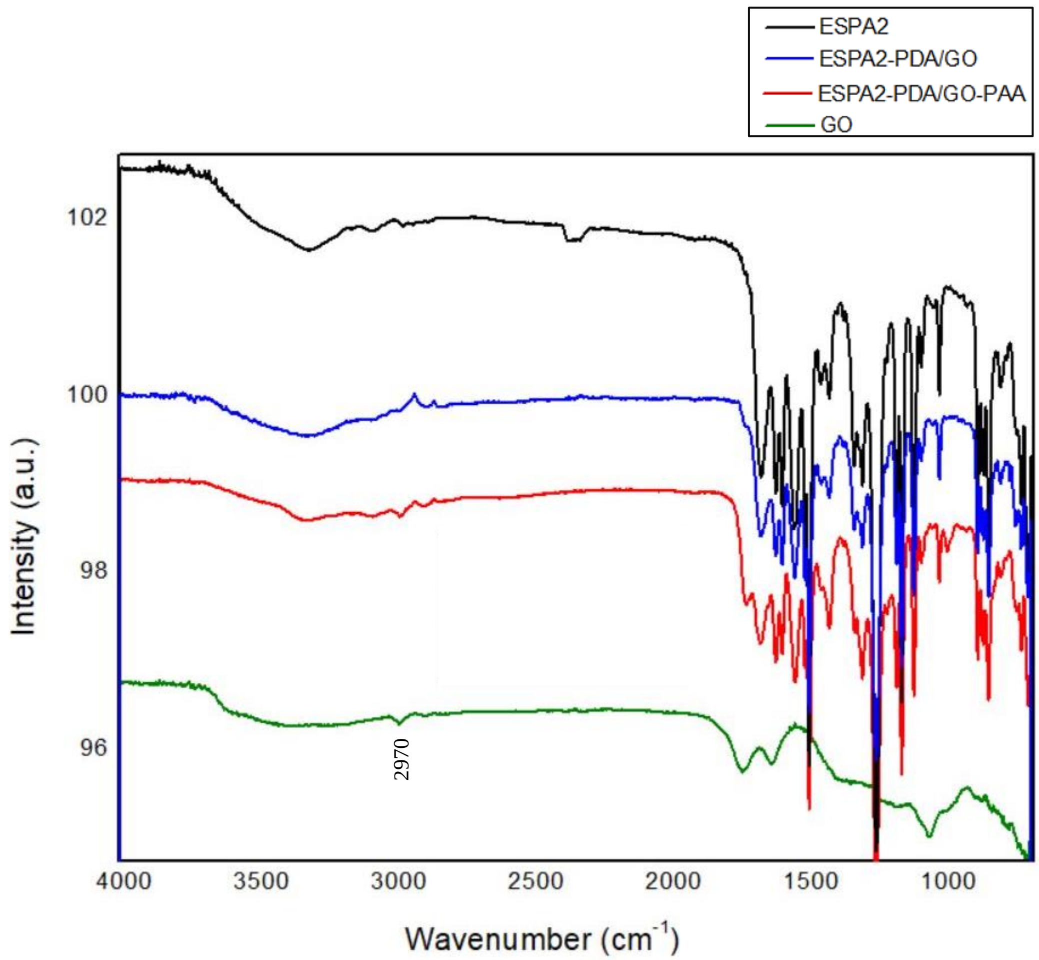

Figure 17: FTIR spectroscopy for the low wavenumber section of the spectrum for the ESPA2 membrane for Synthesis Two through the addition of polyacrylic acid (PAA) with control samples.

The peak at 2970 cm^{-1} on the ESPA2-PDA/GO-PAA curve mirrors the peak on the GO curve suggesting that GO is attached to the membrane sample. The inverted peak for the ESPA2-PDA/GO sample is most likely a result of issues with the background reading.

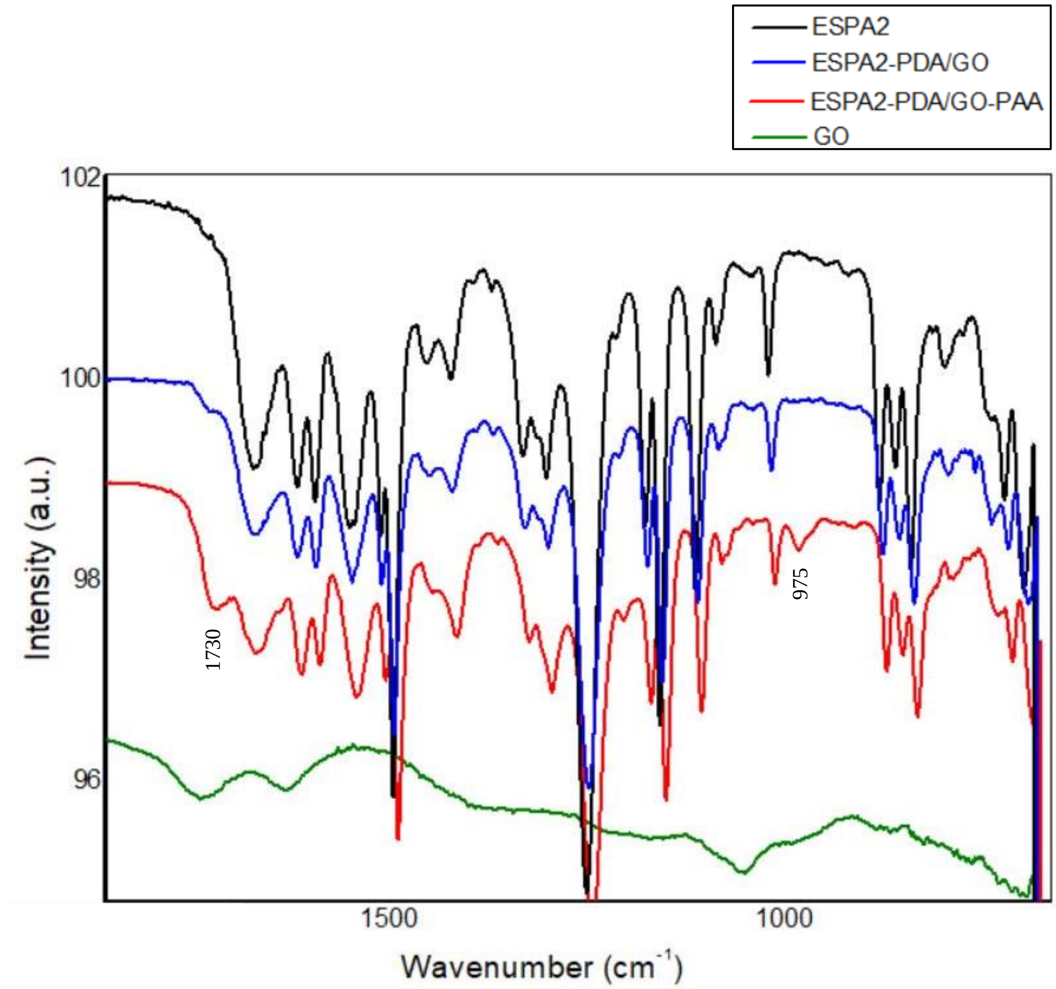

Figure 18: Enlarged view of the low wavenumber section of Figure 17.

New peaks appear at 1730 and 975 cm^{-1} for the membrane sample that underwent Synthesis Two through the addition of PAA. The peak at 1730 cm^{-1} corresponds to the carboxylic groups that compose the side chains of PAA and are also present in GO. The peak was present when the membrane has been modified with PDA and GO, and intensity increased with the inclusion of PAA and its additional carboxylic groups. The appearance of the peak at 975 may represent the addition of numerous alkoxy (C-O) bonds in PAA. These changes from both the bare membrane and the membrane with PDA and GO attached suggest that polymerization on the GO nanosheets did occur. Permeability tests were needed to determine if the level of polymerization in a one-hour reaction was acceptable. The results of the permeability test along with the earlier test for comparison are shown in Table 3. Once again, these results should be treated as preliminary values.

Table 3: Preliminary permeability data for steps of Synthesis Two through the addition of polyacrylic acid (PAA).

Sample	Polymerization Time	Permeability (L/m^2-h)
ESPA2	---	1286
ESPA2 – PDA	---	1286
ESPA2 – PAA	1 hr	60
ESPA2 – PAA	30 min	86
ESPA2 – PDA – GO	---	1224
ESPA2 – PDA – GO – PAA	1 hr	735
ESPA2 – PDA – GO – PAA	30 min	104

Adding only PAA to the bare membrane with a one-hour polymerization time resulted in a significant reduction in permeability. The reduction was similar, but not quite as extreme, when the time was reduced to 30 minutes. Adding PAA with a one-hour polymerization time to a membrane already modified with PDA and GO resulted in a much lower reduction in permeability. Unexpectedly, shortening the polymerization time to 30 minutes drastically increased the reduction in permeability. The difference may be due to unintended differences in the membrane samples or may have a different cause. Possibilities include that the PDA and GO modification slows polymerization by reducing available sites for the PAA to attach to the membrane surface or that acrylic acid has a lower affinity for GO than for the bare membrane's functional groups. The large reduction in permeability for either modification can be prevented by further limiting the extent of polymerization. Further experiments are needed with a range of polymerization times to determine a length that has an acceptable reduction in permeability while still providing antiscalant properties.

Section 4: Conclusions

Two main syntheses were performed in this study: Synthesis One using EDC and NHS to attach GO to the membrane surface through amination and Synthesis Two using polydopamine to attach GO to the membrane surface. A summary of the key trials is shown in Table 4.

Table 4: Summary of synthesis results.

Synthesis	Details	Result
1	2-minute, 200 ppm NaOCl reaction on ESPA2 membrane	Failure before completion of step 4
1	5-minute, pure NaOCl reaction on ESPA2 membrane	Failure before completion of step 5
2	Through adding polydopamine	Successful
2	Through adding GO	Successful
2	Through adding PAA	Successful

Both versions of Synthesis One, with a two-minute and a five-minute NaOCl reaction, failed to definitively attach GO. The five-minute reaction time with a high NaOCl concentration trial improved upon the two-minute reaction time with a low NaOCl concentration trial most likely due to the reaction having a higher yield, but the improvement was not enough to continue pursuing this synthesis route. Another consideration for transitioning to a new synthesis was that the source of error could not be identified after multiple experiments.

Synthesis Two used a different strategy for attaching the GO to the membrane surface. Following general guidelines from the literature, Synthesis Two was successful in adding PDA, GO, and PAA to the membrane surface. The additions of PDA and GO were evidenced by FTIR, Raman, and confocal spectroscopy and permeability testing data sets. Once GO was believed to be present, the addition of PAA was implemented in the synthesis procedure. The attachment and polymerization of PAA was suggested by FTIR spectroscopy and permeability testing. Although PAA was able to attach to the membrane surface, polymerization proceeded to a greater extent than desired. Further tests must be completed to determine the optimal polymerization time.

References

Cao, B., Ansari, A., Yi, X., Rodrigues, D., & Hu, Y. (2018). Gypsum scale formation on graphene oxide modified reverse osmosis membrane. *Journal of Membrane Science, 552*, 132-143.

Choi, W., Choi, J., Bang, J., & Lee, J.-H. (2013). Layer-by-layer assembly of graphene oxide nanosheets on polyamide membranes for durable reverse-osmosis applications. *ACS Applied Materials & Interfaces, 5*(23), 12510-12519.

Elimelech, M., & Phillip, W. A. (2011). The Future of Seawater Desalination: Energy, Technology, and the Environment. *Science*, *333*(6043), 712–717.

Hegab, H., & Zou, L. (2015). Graphene oxide-assisted membranes: Fabrication and potential applications in desalination and water purification. *Journal of Membrane Science, 484*, 95-106.

Hou, Y., Gao, Y., Li, J., & Xu, X. (2010). Monitoring of CaSo4 deposition behaviors on biofilm during nanofiltration via ultrasonic time-domain reflectometry (UTDR). *Water Science & Technology*, *61*(11), 2853-61.

Kim, S., Ko, S., Kang, K., & Han, J. (2010). Direct seawater desalination by ion concentration polarization. *Nature Nanotechnology, 5*, 297-301.

Li, H., Peng, L., Luo, Y., & Yu, P. (2015). Enhancement in membrane performances of a commercial polyamide reverse osmosis membrane via surface coating of polydopamine followed by the gratfting of polytheylenimine. *RCS Advances*(119), 98566-98575.

Liu, Q., & Xu, G.-R. (2016). Graphene oxide (GO) as functional material in tailoring polyamide thin film (PA-TFC reverse osmosis (RO) membranes. *Desalination, 394*, 162-175.

Liu, S., Xeng, T., Hofmann, M., Burcombe, E., Wei, J., Jiang, R., Kong, J., Chen, Y. (2011). Antibacterial activity of graphite, graphite oxide, graphene oxide, and reduced graphene oxide: Membrane and oxidative stess. *ACS Nano, 5*(9), 6971-6980.

Lyster, E., Kim, M.-M., Au, J., & Cohen, Y. (2010). A method for evaluating antiscalant retardation of crystal nucelation and growth on RO membranes. *Journal of Membrane Science, 364*(1), 122-131.

Matin, A., Khan, Z., Zaidi, S., & Boyce, M. (2011). Biofouling in reverse osmosis membranes for seawater desalination: Phenomena and prevention. *Desalination, 281*, 1-16.

Perreault, F., Tousley, M., & Elimelech, M. (2014). Thin-Film Composite Polyamide Membranes Functionalized with Biocidal Graphene Oxide Nanosheets. *Environmental Science & Technology Letters, 1*(1), 71-76.

Radu, A., Bergwerff, L., van Loosdrecht, M., & Picioreanu, C. (2015). Combined biofouling and scaling in membrane feed channels: a new modeling approach. *Biofouling, 31*(1), 83-100.

Rahaman, S., Therien-Aubin, H., Ben-Sasson, M., Ober, C., Nielsen, M., & Elimelech, M. (2014). Control of biofouling on reverse osmosis polyamide membranes modified with biocidal nanoparticles and antifouling polymer brushes. *Journal of Materials Chemsistry B*, *2*, 1724-1732.

Rao, Z., Feng, K., Tang, B., & Wu, P. (2016). Surface decoration of amino-functionalized metal-organic framework/graphene oxie composite onto polydopamine-coated membrane substrate for highly efficient heavy metal removal. *Applied Materials & Interfaces*, *9*(3), 2594-2605.

Shannon, M., Bohn, P., Elimelech, M., Georgiadis, J., Marinas, B., & Mayes, A. (2008). Science and technology for water purification in the coming decades. *Nature, 452*(7185), 301-310.

Sweity, A., Oren, Y., Ronen, Z., & Hersberg, M. (2013). The influence of antiscalants on biofouling of RO membranes in seawater desalination. *Water Research, 47*(10), 3389-3398.

Xu, G.-R., Wang, J.-N., & Li , C.-J. (2013). Strategies for improving the performance of the polyamide thin film composite (PA-TFC) reverse osmosis (RO) membranes: Surface modifications and nanoparticles incorporations. *Desalination, 328*, 83-100.

Zhang, W., Jia, J., Qiu, Y., & Pan, K. (2018). Polydopamine-grafted graphene oxide composite membranes with adjustable nanochannels and separation performance. *Advanced Materials Interfaces, 5*(8).

Appendices

Additional Data

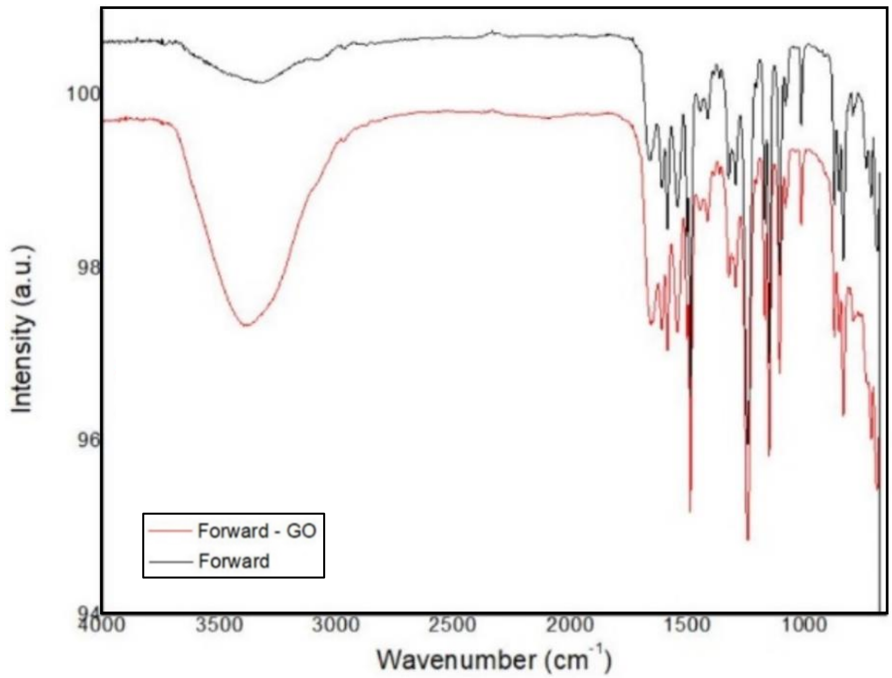

Figure 19: FTIR spectroscopy for Synthesis One using a forward osmosis membrane.

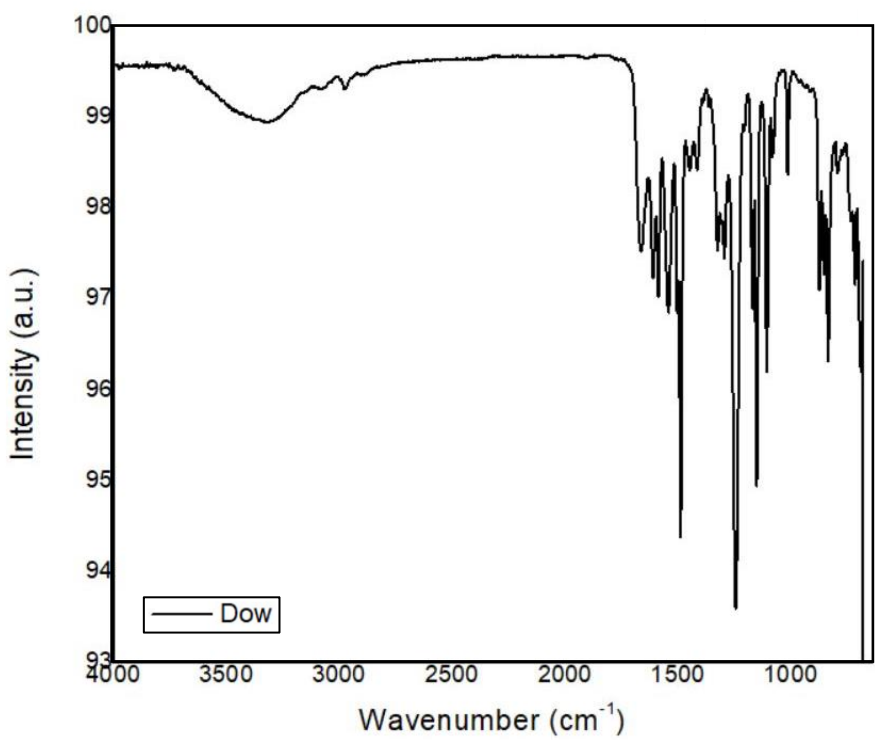

Figure 20: FTIR spectroscopy for Synthesis One using a reverse osmosis membrane from Dow.

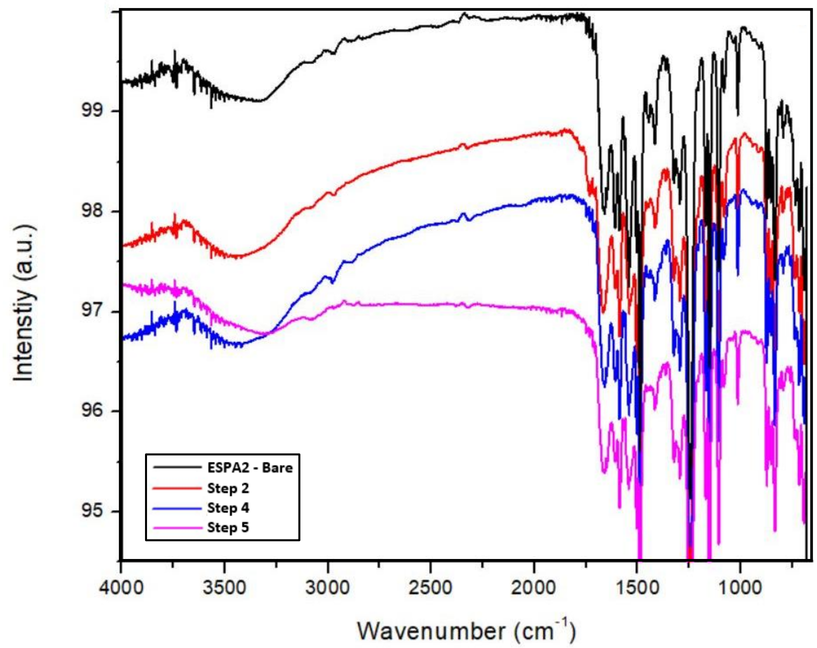

Figure 21: Entire spectrum corresponding to Figure 11.

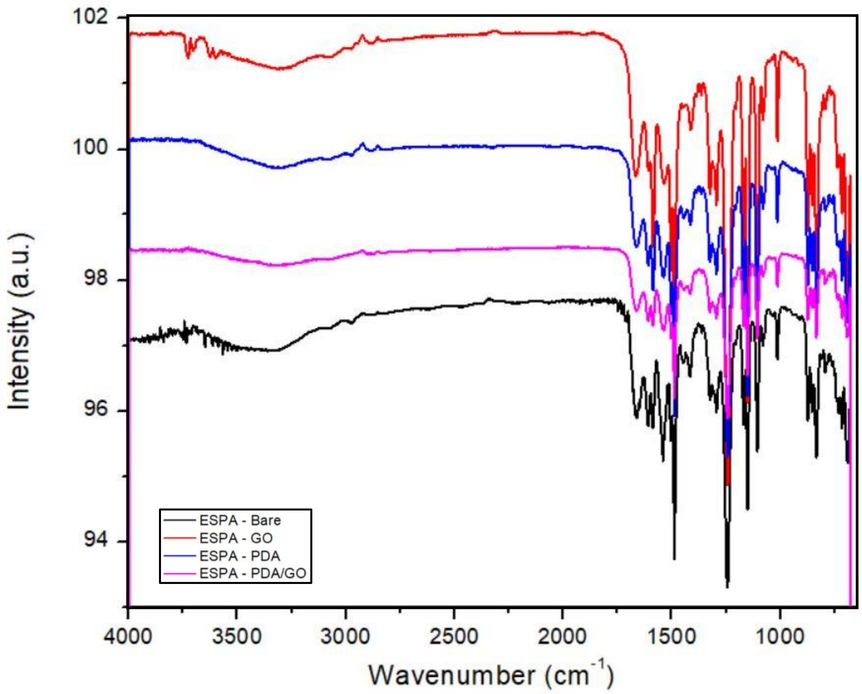

Figure 22: Entire spectrum corresponding to Figure 13.